The Effect of Ceramide on Phosphatidylcholine Membranes: A Deuterium NMR Study

Ya-Wei Hsueh,* Ralph Giles,* Neil Kitson,‡ and Jenifer Thewalt*†
Departments of *Physics and †Molecular Biology and Biochemistry, Simon Fraser University, Burnaby, British Columbia V5A 1S6; and ‡Department of Medicine, Division of Dermatology, University of British Columbia, Vancouver, British Columbia V5Z 4E8, Canada

ABSTRACT Biological membranes contain domains having distinct physical properties. We study defined mixtures of phosphoglycerolipids and sphingolipids to ascertain the fundamental interactions governing these lipids in the absence of other cell membrane components. By using ^{2}H-NMR we have determined the temperature and composition dependencies of membrane structure and phase behavior for aqueous dispersions of 1-palmitoyl-2-oleoyl-*sn*-glycero-3-phosphocholine (POPC) and the ceramide (Cer) *N*-palmitoyl-sphingosine. It is found that gel and liquid-crystalline phases coexist over a wide range of temperature and composition. Domains of different composition and phase state are present in POPC/Cer membranes at physiological temperature for Cer concentrations exceeding 15 mol %. The acyl chains of liquid crystalline phase POPC are ordered by the presence of Cer. Moreover, Cer's chain ordering is greater than that of POPC in the liquid crystalline phase. However, there is no evidence of liquid-liquid phase separation in the liquid crystalline region of the POPC/Cer phase diagram.

INTRODUCTION

It is now widely accepted that cell membranes are complex entities containing distinct, long-lived domains differing in composition and physical characteristics. These specialized patches include "rafts," detergent-insoluble glycosphingolipid-enriched domains (DIGs), and caveolae. Although these types of patches differ in protein and lipid content, they share the characteristic of being enriched in cholesterol and in lipids (such as sphingolipids) that have high gel-to-liquid-crystalline transition temperatures. Regulation of sphingolipid levels in cells is complex and has significant consequences. For example, acid sphingomyelinase activity producing elevated ceramide (Cer) concentrations is associated with apoptosis in vivo (Kirschnek et al., 2000). For recent reviews of the evidence linking the formation of Cer-enriched patches in membranes to Cer's role as a second messenger in signaling pathways, see Venkataraman and Futerman (2000) and Dobrowsky (2000). A crucial component governing the interaction of these Cer-enriched domains with downstream targets may be the distinct physical properties such domains are thought to possess.

Our particular interest (Kitson et al., 1994; Bouwstra et al., 1997) has been in the role of Cer in determining the physical properties of the barrier-forming intercellular lamellae found in the outermost layer of the epidermis. Ceramide is a major component of these lipid layers, and we and others (e.g., Pilgram et al., 1999) have shown that even in the presence of significant mole fractions of cholesterol, Cer confers very unusual physical properties on these membranes, forming regions that are crystalline in nature: in essence, "extreme" domains.

Acknowledging that these intercellular "barrier" lamellae are unusual biological membranes, we wondered about the influence of Cer on the physical properties of more conventional membranes (Giles and Thewalt, 1999), especially given Cer's important biological effects. Studies describing Cer's effects on the physical properties of model membranes are as yet relatively rare. Cer, even in the absence of other lipids, presents challenges to those seeking insight into its structure due to complex time-dependent hydration behavior and its very high order-disorder phase transition temperature of 80–93°C (Shah et al., 1995; Moore et al., 1997; Rerek et al., 2001). In model membranes composed of phosphatidylcholine (PC), sphingomyelin, and cholesterol in various proportions, Cer is reported, based on fluorescence measurements, to "strongly promote domain formation" (Xu et al., 2001) and to increase acyl chain order (Massey, 2001). Also, Cer has been found to cause microdomain formation or phase separation in saturated PC membranes (Carrer and Maggio, 1999; Huang et al., 1998; Holopainen et al., 1997, 2000). Cer's effects on 1-palmitoyl-2-oleoyl-*sn*-glycero-3-phosphocholine (POPC) membranes are less well understood; recent studies have reported, for example, that POPC and Cer mix well (Massey, 2001) or conversely that Cer induces microdomains in POPC (Holopainen et al., 1998).

We chose POPC as a well-studied and natural "host" phospholipid in which to investigate the influence of Cer. Using the direct, unambiguous, and quantitative information provided by deuterium NMR, we present here a comprehensive examination of Cer's effects on membrane phase state and acyl chain order. The Cer used was pure synthetic *N*-palmitoyl-sphingosine, and the palmitoyl chain of each lipid was deuterated in turn. The analysis of NMR spectra as functions of temperature and composition (to a maximum

Submitted November 8, 2001, and accepted for publication January 31, 2002.

Address reprint requests to Jenifer Thewalt, 8888 University Drive, Burnaby, BC V5A 1S6, Canada. Tel.: 604-291-3151; Fax: 604-291-3592; E-mail: jthewalt@sfu.ca.

0006-3495/02/06/3089/07 $2.00

concentration of 25 mol % Cer) allowed the determination of a detailed partial phase diagram of POPC/Cer.

MATERIALS AND METHODS

POPC-d31 was obtained from Avanti Polar Lipids, Inc. (Alabaster, AL). POPC, Cer-d31, and Cer were obtained from Northern Lipids (Vancouver, BC). Deuterium-depleted water was from Sigma-Aldrich Canada, Inc. (Oakville, ON). POPC-d31 and Cer (or POPC and Cer-d31) were mixed in the appropriate quantities, dissolved in benzene/methanol, 4:1 (v/v) and then freeze-dried. Samples were hydrated using a pH 7.4 buffer prepared in deuterium-depleted water containing 50 mM HEPES, 120 mM NaCl, 4 mM EDTA. Hydration was performed by freeze-thaw-vortex cycling five times between liquid nitrogen temperature and 85°C.

^{2}H-NMR experiments were performed on a locally built spectrometer at 46.8 MHz using the quadrupolar echo technique (Davis et al., 1976). The typical spectrum resulted from 10,000 to 15,000 repetitions of the two-pulse sequence with 90° pulse lengths of 3.95 μs, interpulse spacing of 40 μs, and a dwell time of 2 μs. The delay between acquisitions was 300 ms to 5 s and data were collected in quadrature with Cyclops 8-cycle phase cycling. The spin-lattice relaxation time, T_1, was measured using the saturation recovery technique. The sample was heated from −15°C to 69°C. At each temperature the sample was allowed to equilibrate for 20 min before a measurement.

The first moment, M_1, was calculated using

$$M_1 = \frac{1}{A} \sum_{\omega=-x}^{x} |\omega| \, f(\omega) \qquad (1)$$

where ω is the frequency shift from the central (Larmor) frequency, $f(\omega)$ is the spectral intensity, and

$$A = \sum_{\omega=-x}^{x} f(\omega).$$

The boundaries of the gel-liquid crystalline coexistence region are determined by the spectral subtraction method, which was first applied to PC/cholesterol membranes (Vist and Davis, 1990; Thewalt and Bloom, 1992) and has also been used to investigate PC/cerebroside phase equilibria (Lu et al., 1993). Within the two-phase region, each observed spectrum is simply a linear combination of the spectra typical for gel and liquid-crystalline (lc) phases at the gel phase and lc phase boundaries, respectively, at the same temperature. The relative amount of gel and lc components is determined by the sample composition. Given two area-normalized observed spectra from samples of different composition at the same temperature, the typical spectra for the lc (or gel) phase at the lc (or gel) phase boundary can be obtained by subtracting a fraction of one spectrum from the other. The phase boundaries then can be calculated using the lever rule.

The C—D bond order parameter, S_{CD}, is related to the quadrupolar splitting $\Delta\nu$ from a de-Paked spectrum according to $\Delta\nu = \frac{3}{2}(e^2qQ/h)S_{CD}$, where $(e^2qQ/h) = 167$ kHz is the static quadrupolar coupling constant (Davis and Jeffrey, 1977). The smoothed order parameter profiles were determined from the de-Paked spectra using a procedure described by Lafleur et al. (1989). This approach assumes monotonic decrease of the order along the acyl chain and therefore reproduces only the smoothed features of the order variation. To verify that the smoothed order parameter calculation was valid for Cer-d31, the temperature-dependence of all individually resolved doublets was monitored. All behaved similarly, the splittings narrowing gradually as temperature was increased. This indicates that the average conformation of all methylene groups along the Cer-d31 palmitoyl chain is equivalent, namely perpendicular to the membrane normal. (If a "kink" were present, like the kink near the ester bond on the sn-2 chain of PC, for example, the temperature-dependence of the *splitting corresponding to the deuterons at the kink would have a much smaller slope.)*

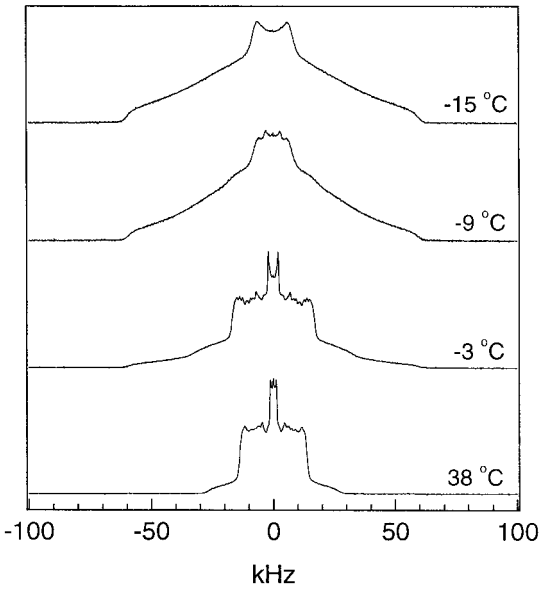

FIGURE 1 ^{2}H-NMR spectra of 85:15 POPC-d31/Cer as a function of temperature.

RESULTS AND DISCUSSION

POPC-d31/Cer and POPC/Cer-d31 multilamellar dispersions were prepared for Cer (or Cer-d31) concentrations of 0, 10, 15, 20, and 25 mol %. ^{2}H-NMR spectra were collected from −15°C to 69°C. The POPC-d31/Cer system undergoes a broad transition from a gel phase to an lc phase as the temperature is raised. As seen in Fig. 1, 85:15 POPC-d31/Cer displays gel phase spectra below −10°C. Above 38°C, the spectra indicate that POPC is in the lc phase. The lineshape is a superposition of Pake doublets, implying that the lipid acyl chain undergoes rapid, axially symmetric reorientation about the bilayer normal. Between −10°C and 38°C, both gel and lc spectral components were seen in the spectrum, indicating the coexistence of gel and lc phases. The center of the spectrum at 38°C exhibits an isotropic peak having ~0.4% of the total intensity. This peak's intensity increases linearly with temperature, reaching ~1% at 69°C; thus we attribute it to a small amount of vesicle budding (Nezil et al., 1992).

Fig. 2 shows the spectrum of POPC-d31/Cer as a function of Cer concentration at −5°C. At −5°C, pure POPC displays an lc spectrum. For 90:10 POPC-d31/Cer a small gel component appears in the spectrum, as indicated by the presence of intensity beyond ~±35 kHz. The coexistence of gel and lc phases in the spectrum indicates that Cer induces gel-phase domains (phase separation) in the POPC-d31 bilayer. Gel-phase domains induced by Cer have also been observed in saturated PC membranes, such as dipalmi-

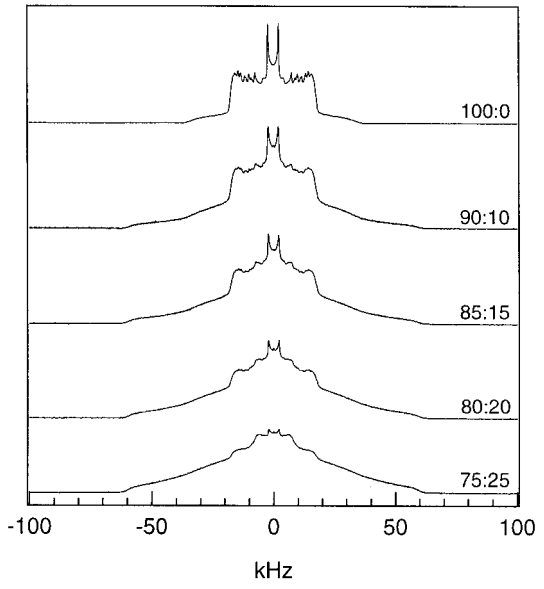

FIGURE 2 ^{2}H-NMR spectra of POPC-d31/Cer as a function of Cer concentration at $T = -5°C$.

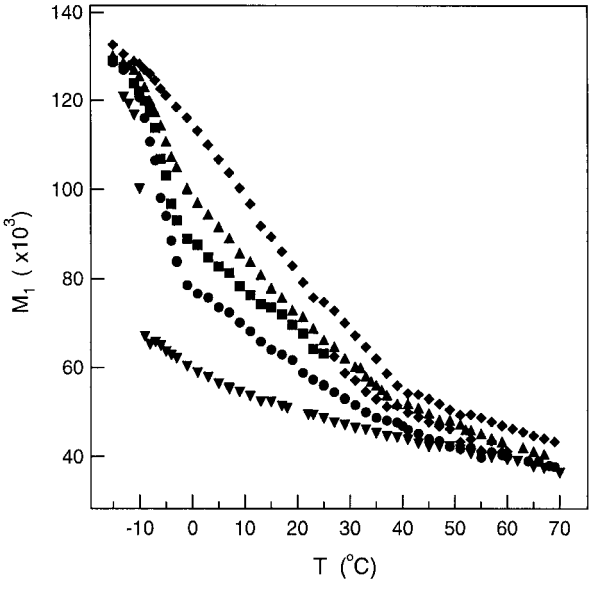

FIGURE 3 The temperature dependence of M_1 for POPC-d31/Cer. ▼, pure POPC-d31; ●, 90:10 POPC-d31/Cer; ■, 85:15 POPC-d31/Cer; ▲, 80:20 POPC-d31/Cer; ♦, 75:25 POPC-d31/Cer.

toylphosphatidylcholine (DPPC) (Huang et al., 1998) and dimyristoylphosphatidylcholine (DMPC) (Holopainen et al., 2000). The coexistence of gel and lc spectral components is more apparent for 85:15 POPC-d31/Cer, and as the Cer concentration is raised to 25 mol % the proportion of gel component increases further. Concomitantly, the proportion of liquid crystalline component decreases, shown by the reduction of the spectral intensity at ±18 kHz. Therefore, Cer enhances tight chain packing in POPC bilayers. Moreover, as will be discussed later, the lc component becomes broader with increasing Cer concentration, implying more motional restriction for the POPC acyl chains as more Cer is added to the mixture.

The variation of the first moment, M_1, with temperature measures changes in average spectral width and thus reflects phase changes in the membrane. Fig. 3 shows the temperature-dependence of M_1 for dispersions of POPC-d31/Cer. As seen in Fig. 3, pure POPC-d31 undergoes a sharp transition from the gel to the lc phase, as indicated by the drastic drop in M_1 at $T = -10°C$. In contrast, in the presence of 10–25 mol % Cer, POPC-d31 displays a much broader transition, with a gradual decrease in M_1. The coexistence of gel and lc phases is observed over a wide range of temperature and composition. Furthermore, M_1 versus T curves of 10, 15, and 20 mol % Cer display a change of slope near −3°C. As we will discuss later, this change of slope is in fact associated with the incorporation of Cer into the POPC lc phase.

In Fig. 4 the variation of M_1 with temperature for membranes composed of 90:10 POPC/Cer is shown. Both lipids, in turn, were ^{2}H-labeled, and it is clear that the phase transition behavior exhibited by POPC-d31 and Cer-d31 are quite different. The POPC-d31 component of the membrane begins to melt at −10°C, transforming from gel to gel/lc coexistence (see Fig. 5 *A*). However, the Cer-d31 component is still in the gel phase, as indicated both by the value of its M_1 in Fig. 4 and its gel phase spectrum in Fig. 5 *E*. Thus, the lc phase seen between −10°C and −3°C is a pure POPC-d31 lc phase. Cer-d31 does not begin to melt until −3°C, where a small drop in M_1 occurs. Above −3°C, an

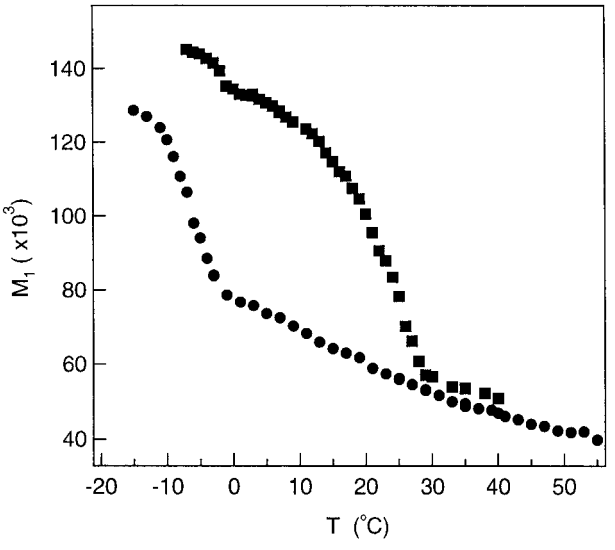

FIGURE 4 M_1 as a function of temperature for ■, 90:10 POPC/Cer-d31 and ●, 90:10 POPC-d31/Cer. Here we have shifted the M_1 of 90:10 POPC/Cer-d31 by −2°C, given the fact that POPC (or POPC-d31) is the major component in 90:10 POPC/Cer and POPC chain deuteration downshifts the transition temperature by 2°C.

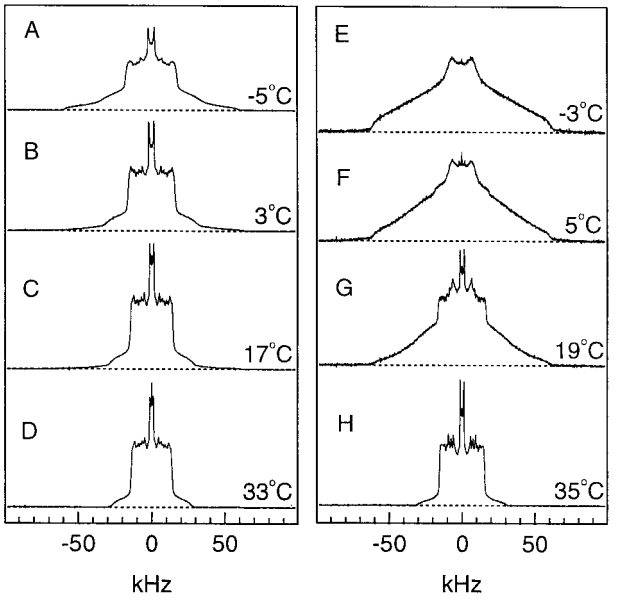

FIGURE 5 ^{2}H spectra as a function of temperature for (*A–D*) 90:10 POPC-d31/Cer and (*E–H*) 90:10 POPC/Cer-d31.

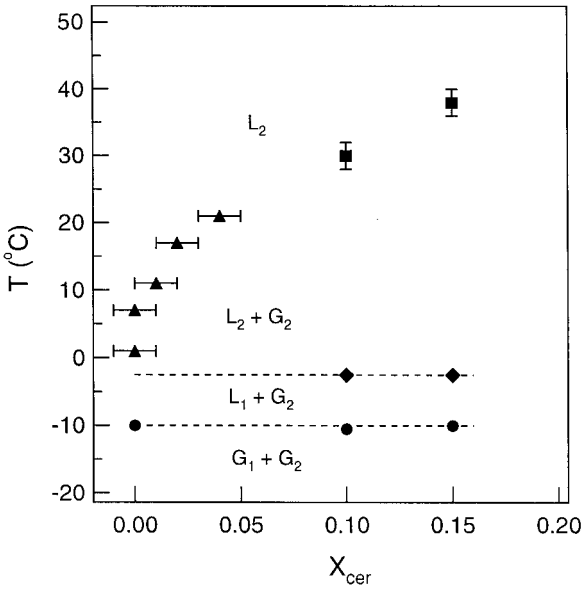

FIGURE 6 Partial phase diagram of the POPC/Cer membrane. ■, obtained by inspection of spectra; ● and ◆, obtained by inspection of M_1 curves (errors are within the symbol); ▲, obtained from spectral subtraction. Refer to the text for the definition of G_1, G_2, L_1, and L_2.

lc component is present in Cer-d31 spectra (see Fig. 5, *F* and *G*), indicating the participation of Cer-d31 in the predominantly POPC lc phase domain. However, the POPC-d31 and Cer-d31 spectra in Fig. 5, *B* and *F*, respectively, show that ~70% of the POPC-d31 is in the lc phase and ~90% of the Cer-d31 is in the gel phase. Although domains of both phases are primarily composed of POPC, the fraction of Cer in the gel domains is much larger than that in the lc phase domains; thus the gel phase domains are rich in Cer, while the lc phase domains are poor in Cer. The ^{2}H-labeled Cer in 90:10 POPC/Cer-d31 completes the transformation to the lc phase at 30 ± 2°C, as indicated by the M_1 curve in Fig. 4. By inspection, the gel component of 90:10 POPC-d31/Cer also completely disappears at this temperature. In summary, although the POPC and Cer components of mixed POPC/Cer membranes undergo gel/(gel + lc) melting at different temperatures, they complete the conversion to the lc phase at the same temperature.

The partial phase diagram derived from the above characteristic temperatures and the corresponding lipid compositions is shown in Fig. 6. For low Cer concentrations, aqueous dispersions of POPC/Cer may be treated as a two-component system, assuming that water concentration does not influence phase behavior. Therefore the line at −10°C, which is essentially independent of the Cer concentration up to $X_{cer} = 0.15$, implies three-phase coexistence and suggests a gel-gel immiscibility at lower temperatures. Below −10°C a pure POPC gel phase domain, G_1, is immiscible with a POPC/Cer gel phase domain, G_2. Above −10°C, POPC begins to melt. A pure POPC lc phase, L_1, coexists with G_2. The horizontal line at −3°C, determined from the changes of slope in M_1 versus temperature curves of POPC-d31/Cer (Fig. 3), is the $L_1 + G_2/L_2 + G_2$ boundary, where L_2 denotes the POPC/Cer lc phase. Above −3°C, Cer begins to melt and becomes incorporated into the previously pure POPC lc phase. The lipid dispersions display $L_2 + G_2$ phase coexistence, i.e., Cer-rich gel phase domains coexist with Cer-poor lc phase domains. Note that at physiological temperature gel domains are present for Cer concentrations of only 15 mol %. The liquidus curve, determined by inspection of the POPC and Cer spectra and M_1 curve of Cer, as well as spectral subtraction, is strongly dependent on the Cer concentration. The agreement between observations based on POPC/Cer multilamellar dispersions labeled with either POPC-d31 or Cer-d31 indicates that POPC and Cer mix well in the lc phase.

For $X_{cer} \geq 0.2$ the phase composition of POPC/Cer is complicated. A solid (or crystalline) phase is present in the Cer spectrum. This solid phase has a much longer spin-lattice relaxation time ($T_1 \approx 2$ s) than lc and gel phases. The existence of the solid phase can be verified by using a longer repetition time, for example 5 s, in the quadrupolar echo pulse sequence. Fig. 7 *B* shows the difference between spectra of 75:25 POPC/Cer-d31 obtained at repetition times of 5 and 0.3 s. The signal intensity beyond ~±20 kHz displays a shoulder-like shape with edges at ±63 kHz, an indication of the solid phase. Fig. 7 *C* shows the difference between the spectra of pure hydrated Cer-d31 obtained at repetition times of 5 and 0.3 s at the same temperature where pure Cer-d31 displays the solid phase. The lineshape beyond ~±20 kHz is quite similar to that in Fig. 7 *B*, confirming the presence of the solid phase in 75:25 POPC/

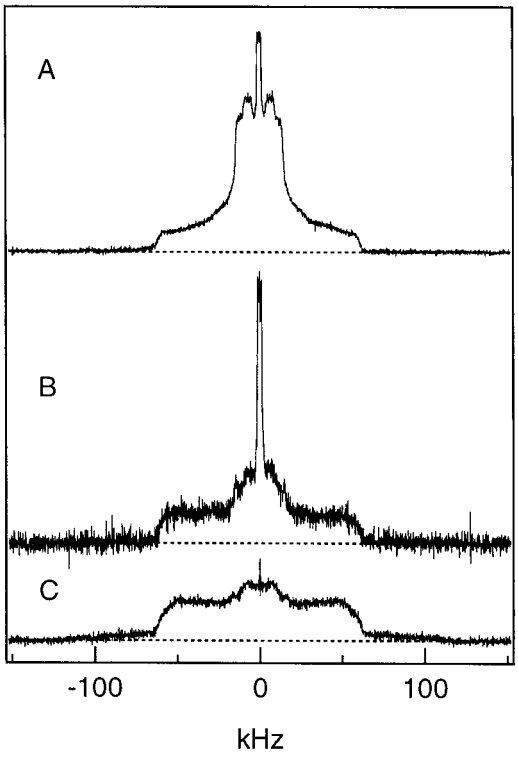

FIGURE 7 ^{2}H spectra for 75:25 POPC/Cer-d31 obtained at 47°C using (*A*) a repetition time of 0.3 s. (*B*) the difference between the spectrum taken at repetition times of 5 and 0.3 s. Note that the enhanced narrow central region is due to the CD_3 resonances, which typically have longer T_1 values than those of the methylene groups. (*C*) The difference between spectra taken at repetition times of 5 and 0.3 s for pure hydrated Cer-d31 at 47°C.

Cer-d31. The solid phase was also observed in the Cer spectra of 80:20 POPC/Cer-d31, but the amount of solid was much less than in 75:25 POPC/Cer-d31. Because POPC spectra of 80:20 POPC-d31/Cer and 75:25 POPC-d31/Cer do not contain any solid component, the solid phase seen in these two membranes is pure Cer.

As seen in Fig. 7 *A*, in addition to the solid phase, the Cer spectrum also contains lc and gel phases. This coexistence of three phases is observed at $T = 25$°C and 47°C in 80:20 POPC/Cer-d31 and 75:25 POPC/Cer-d31, hinting at a three-phase area in the phase diagram. The proportion of solid phase and the spectrum change slightly with time, indicating that the phase composition changes with time. The observation of the three-phase area violates the Gibbs phase rule for a two-component system in equilibrium, where a three-phase region can only be a line. Together with the time-dependent phase composition, we conclude that the aqueous dispersions of 80:20 POPC/Cer and 75:25 POPC/Cer are metastable. Some sphingolipids are known to exhibit metastable behavior (Freire et al., 1980; Ruocco et al., 1981; Curatolo, 1982). For example, a metastable bilayer phase is observed in hydrated *N*-palmitoyl-sphingosine that is interconvertible with a stable bilayer phase (Shah et al., 1995). A dehydrated metastable crystal form that is interconvertible with a hydrated stable crystal form is also reported for hydrated cerebroside (Ruocco et al., 1981). These complex behaviors are observed particularly at partial or intermediate degrees of hydration (Maggio et al., 1985). We propose that when Cer is present above a threshold concentration of ~20 mol % in the POPC membrane, the aqueous POPC/Cer dispersion must be treated as a three-component system, i.e., water can no longer be treated as a "silent" third component. To avoid these hydration complexities we have focused on the phase diagram at low Cer concentrations, where solid Cer is not in evidence. The phase diagram in Fig. 6 therefore represents completely hydrated POPC/Cer membranes.

The liquidus between 0 and 30°C was obtained using the spectral subtraction method on membranes containing 10 and 15 mol % Cer. However, spectral subtraction is generally applied to a two-phase region bordered by boundaries defining single-phase regions. The phase diagram in Fig. 6 implies that only one boundary (liquidus) can be well defined. The phase composition at higher Cer concentrations ($X_{cer} \geq 0.2$) is complicated, as mentioned earlier, due to the presence of solid Cer. To apply spectral subtraction to this system, we treated the solid Cer as "invisible" because it does not mix with POPC. Thus, we define an effective Cer concentration, $X'_{cer} = (n_{cer} - n_{cer(solid)})/(n_{POPC} + n_{cer} - n_{cer(solid)})$, where n_{cer} (n_{POPC}) is the total number of moles of Cer (POPC), and $n_{cer(solid)}$ is the number of moles of Cer in the solid phase. Thus, presumably we have lc $\rightarrow$ lc + gel $\rightarrow$ gel in the X'_{cer} phase diagram, and then the spectral subtraction method can be applied. The effective liquidus X_f' and solidus X_g' can be obtained from the spectral subtraction equations. Because there is no solid at low Cer concentration, X_f' in the X'_{cer} phase diagram corresponds exactly to the liquidus X_f in the X_{cer} phase diagram (note, $X_{cer} = n_{cer}/(n_{POPC} + n_{cer})$), i.e., $X_f' = X_f$. In Fig. 6, X_f' matches well with those points obtained from direct examination of spectra and the temperature-dependence of M_1, showing the validity of our calculation. As mentioned earlier, due to the complicated phase behavior at high Cer concentration, only the liquidus is well defined. Thus we cannot derive the solidus X_g from the effective solidus X_g' (which ranged from 0.26 to 0.38).

The partial phase diagram of a POPC/Cer membrane (Fig. 6) is similar to the dioleoylphosphatidylcholine/dipalmitoylphosphatidylethanolamine (DOPC/DPPE) phase diagram (Wu and McConnell, 1975) at low DPPE concentration. DOPC/DPPE membranes display a horizontal solidus line at low temperature and low DPPE concentration. A second horizontal line is observed at much higher temperature, corresponding to the boundary of $L_1 + G_2/L_2 + G_2$ in Fig. 6. The liquidus curve, corresponding to the boundary of $L_2 + G_2/L_2$ in Fig. 6, is also strongly dependent on the concentration of DPPE. DOPC is analogous to POPC, as both phospholipids have the same headgroup and both are unsaturated lipids with transition temperatures below 0°C.

Also, the case can be made that DPPE is analogous to Cer, as both have small headgroups capable of forming hydrogen bonds, similar chain length, and transition temperatures well above room temperature. Thus, POPC/Cer and DOPC/DPPE do share some common features: the counterparts in each lipid mixture are similar in shape and the transition temperatures of the components in each mixture are quite far apart. If these factors are important determinants of phase behavior, it is not surprising that POPC/Cer and DOPC/DPPE display similar phase diagrams. The facts that Cer is a sphingolipid and does not contain a phosphate group are apparently less important to the lipid/lipid interactions governing the topology of the phase diagram.

There have been some studies on other phospholipid/Cer mixtures. The gel-fluid transition of dielaidoylphosphatidylethanolamine (DEPE)/Cer detected by DSC displays several components (low-T_m and high-T_m components) under the endotherm peak (Veiga et al., 1999). Together with IR data indicating that Cer melts at higher temperatures than the phospholipid, they concluded that the low-T_m component corresponds to the transition of domains rich in phospholipid and the high-T_m component corresponds to the transition of Cer-rich domains, consistent with our observations on POPC/Cer. DSC studies of DPPC/Cer yield similar observations (Carrer et al., 1999). Moreover, like POPC/Cer membranes, DPPC/Cer displays gel-gel immiscibility, but miscibility in the lc phase.

What is the driving force behind Cer-enriched gel domain formation? Some suggest that a hydrophobic mismatch between Cer and PC is the major contribution (Holopainen et al., 1997), while others point out that Cer's lack of a bulky headgroup is of prime importance (Huang et al., 1999). In the POPC/Cer system the chain lengths of POPC and Cer are similar, so hydrophobic mismatch is not important. Since we observed Cer-enriched gel phase domains, this implies that hydrophobic mismatch cannot be the sole driving force of domain formation. Cer's headgroup is small and also has an unusually low hydration capacity compared to phospholipids: these factors are likely to enhance Cer's propensity for gel phase packing.

The order parameter profiles are shown in Fig. 8 for the liquid crystalline phase of POPC/Cer. S_{CD} is defined as $S_{CD} = \frac{1}{2}\langle 3\cos^2\theta_{CD} - 1\rangle$, where θ_{CD} denotes the instantaneous angle between the C—D bond and the direction of the bilayer normal, and the brackets denote orientational averaging on the NMR time scale (typically $\sim 10\ \mu s$). For acyl chains in the all-*trans* configuration, $|S_{CD}| = 0.5$; $|S_{CD}| < 0.5$ if the chain is disordered due to *trans-gauche* conformational isomerizations. Thus, S_{CD} provides a measurement of the degree of orientational order along the lipid acyl chain. In the POPC-d31/Cer and POPC/Cer-d31 dispersions studied, the order parameter distribution along the acyl chain decreases gradually near the headgroup region (bilayer surface) and decreases relatively fast close to the methyl terminal (bilayer interior). This is the typical order profile of the lamellar lc phase. Adding increasing concentrations of Cer to the membrane causes significant and progressive increases to the order parameters of POPC-d31 at all carbon positions along the palmitoyl chain, as shown in Fig. 8. Also, Fig. 8 compares the order profiles of Cer-d31 in the lc phase with those of POPC-d31. The $|S_{CD}|$ of the labeled Cer, for example, 90:10 POPC/Cer-d31, is larger than that of labeled POPC, namely 90:10 POPC-d31/Cer, for all carbon positions, indicating that in the lc phase the acyl chain is more ordered in Cer than in POPC. This might be attributed to the small headgroup of the Cer molecule, which allows for closer chain interactions compared to the POPC molecules. Importantly, the possibility of liquid-liquid phase separation has been disproved by the partial phase diagram.

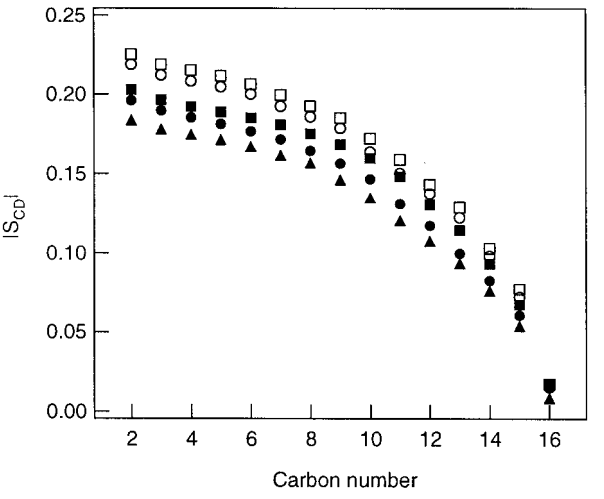

FIGURE 8 Smoothed order parameter profiles $|S_{CD}|$ at 57°C from ▲, pure POPC-d31; ●, 90:10 POPC-d31/Cer; ○, 90:10 POPC/Cer-d31; ■, 85:15 POPC-d31/Cer; □, 85:15 POPC/Cer-d31.

CONCLUSIONS

Summarizing the direct evidence obtained from ^{2}H-NMR concerning the influence of 0–20 mol % Cer on POPC membranes: 1) at low temperatures, POPC/Cer membranes display gel-gel immiscibility; 2) the POPC/Cer gel phase melts at a higher temperature than the POPC gel phase; 3) gel/liquid-crystalline phase coexistence occurs over a wide range of temperature and composition. This implies that Cer-rich gel domains and Cer-poor lc domains are present in the membrane; 4) in the lc phase POPC and Cer mix well, and Cer increases the order in POPC bilayers. Order parameter profiles reveal that Cer chains are more ordered than POPC chains even though both lipids are in the lc phase. Model membranes containing concentrations of Cer >20 mol % present great challenges experimentally due to the appearance of a metastable solid Cer phase.

While it is, of course, risky to apply conclusions reached from studying well-defined model membranes directly to cell membranes, it is possible that acid sphingomyelinase activation could produce high local concentrations of ceramide in membranes in vivo. If the membrane remains in the lc state the effect of Cer would likely be to order the acyl chains, thereby thickening the membrane and changing the curvature energy. If the localized Cer production exceeds the capacity of the lc membrane to accommodate Cer, it is probable that membrane properties would change dramatically due to the formation of gel-like or crystalline domains.

Of particular interest is the influence of cholesterol on the physical properties of membranes containing Cer. How will the liquid-ordered phase that is present in cholesterol-enriched PC membranes be modified by the addition of Cer? Our preliminary results (Y.-W. Hsueh, unpublished results) indicate that low concentrations of Cer dispersed in a 60:40 POPC/cholesterol model membrane are, except at very low temperatures, in an ordered lc state, while higher concentrations of Cer form solid domains. Certainly the hypothesis that the effect of Cer on membrane physical properties is intimately connected with its biological actions deserves further examination.

We thank Martin Zuckermann for very helpful discussions.

This work was supported by research grants from the Canadian Dermatology Foundation, the UBC Epidermolysis Bullosa Research Fund, and the National Sciences and Engineering Research Council of Canada.

REFERENCES

Bouwstra, J. A., J. L. Thewalt, G. S. Gooris, and C. N. Kitson. 1997. A model membrane approach to the epidermal permeability barrier: an x-ray diffraction study. *Biochemistry.* 36:7717–7725.

Carrer, D. C., and B. Maggio. 1999. Phase behavior and molecular interactions in mixtures of ceramide with dipalmitoylphosphatidylcholine. *J. Lipid Res.* 40:1978–1989.

Curatolo, W. 1982. Thermal behavior of fractionated and unfractionated bovine brain cerebrosides. *Biochemistry.* 21:1761–1764.

Davis, J. H., and K. R. Jeffrey. 1977. The temperature dependence of chain order in potassium palmitate-water. A deuterium NMR study. *Chem. Phys. Lipids.* 20:87–104.

Davis, J. H., K. R. Jeffrey, M. Bloom, M. I. Valic, and T. P. Higgs. 1976. Quadrupolar echo deuteron magnetic resonance spectroscopy in ordered hydrocarbon chains. *Chem. Phys. Lett.* 42:390–394.

Dobrowsky, R. T. 2000. Sphingolipid signalling domains: floating on rafts or buried in caves? *Cell. Signalling.* 12:81–90.

Freire, E., D. Bach, M. Correa-Freire, I. Miller, and Y. Barenholz. 1980. Calorimetric investigation of the complex phase behavior of glucocerebroside dispersions. *Biochemistry.* 19:3662–3665.

Giles, R., and J. L. Thewalt. 1999. Model characterization of the effects of ceramide on the lipid bilayer. *Biophys. J.* 76:356*a*. (Abstr.).

Holopainen, J. M., J. Y. A. Lehtonen, and P. K. J. Kinnunen. 1997. Lipid microdomains in dimyristoylphosphatidylcholine-ceramide liposomes. *Chem. Phys. Lipids.* 88:1–13.

Holopainen, J. M., J. Lemmich, F. Richter, O. G. Mouritsen, C. Rapp, and P. K. J. Kinnunen. 2000. Dimyristoylphosphatidylcholine/C16:0-ceramide binary liposomes studied by differential scanning calorimetry and wide- and small-angle x-ray scattering. *Biophys. J.* 78:2459–2469.

Holopainen, J. M., M. Subramanian, and P. K. Kinnunen. 1998. Sphingomyelinase induces lipid microdomain formation in a fluid phosphatidylcholine/sphingomyelin membrane. *Biochemistry.* 37: 17562–17570.

Huang, H., E. M. Goldberg, and R. Zidovetzki. 1998. Ceramides perturb the structure of phosphatidylcholine bilayers and modulate the activity of phospholipase A_2. *Eur. Biophys. J.* 27:361–366.

Huang, H., E. M. Goldberg, and R. Zidovetzki. 1999. Ceramides modulate protein kinase C activity and perturb the structure of phosphatidylcholine/phosphatidylserine bilayers. *Biophys. J.* 77:1489–1497.

Kirschnek, S., F. Paris, M. Weller, H. Grassme, K. Ferlinz, A. Riehle, Z. Fuks, R. Kolesnick, and E. Gulbins. 2000. CD95-mediated apoptosis in vivo involves acid sphingomyelinase. *J. Biol. Chem.* 275:27316–27323.

Kitson, N., J. Thewalt, M. Lafleur, and M. Bloom. 1994. A model membrane approach to the epidermal permeability barrier. *Biochemistry.* 33:6707–6715.

Lafleur, M., B. Fine, E. Sternin, P. R. Cullis, and M. Bloom. 1989. Smoothed orientational order profile of lipid bilayers by ^{2}H-nuclear magnetic resonance. *Biophys. J.* 56:1037–1041.

Lu, D., D. Singh, M. R. Morrow, and C. W. M. Grant. 1993. Effect of glycosphingolipid fatty acid chain length on behavior in unsaturated phosphatidylcholine bilayer: a ^{2}H-NMR study. *Biochemistry.* 32:290–297.

Maggio, B., T. Ariga, J. M. Sturtevant, and R. K. Yu. 1985. Thermotropic behavior of glycosphingolipids in aqueous dispersion. *Biochemistry.* 24:1084–1092.

Massey, J. B. 2001. Interaction of ceramides with phosphatidylcholine, sphingomyelin and sphingomyelin/cholesterol bilayers. *Biochim. Biophys. Acta.* 1510:167–184.

Moore, D. J., M. E. Rerek, and R. Mendelsohn. 1997. FTIR spectroscopy studies of the conformational order and phase behavior of ceramides. *J. Phys. Chem. B.* 101:8933–8940.

Nezil, F. A., S. Bayerl, and M. Bloom. 1992. Temperature-reversible eruptions of vesicles in model membranes studied by NMR. *Biophys. J.* 61:1413–1426.

Pilgram, G. S. K., A. M. Engelsma-van Pelt, J. A. Bouwstra, and H. K. Koerten. 1999. Electron diffraction provides new information on human stratum corneum lipid organization studied in relation to depth and temperature. *J. Invest. Dermatol.* 113:403–409.

Rerek, M. E., H. Chen, B. Markovic, D. Van Wyck, P. Garidel, R. Mendelsohn, and D. J. Moore. 2001. Phytosphingosine and sphingosine ceramide headgroup hydrogen bonding: structural insights through thermotropic hydrogen/deuterium exchange. *J Phys. Chem. B.* 105: 9355–9362.

Ruocco, M. J., D. Atkinson, D. M. Small, R. P. Skarjune, E. Oldfield, and G. G. Shipley. 1981. X-ray diffraction and calorimetric study of anhydrous and hydrated N-palmitoylgalactosylsphingosine (cerebroside). *Biochemistry.* 20:5957–5966.

Shah, J., J. M. Atienza, R. I. Duclos, Jr., A. V. Rawlings, Z. Dong, and G. G. Shipley. 1995. Structural and thermotropic properties of synthetic C16:0 (palmitoyl) ceramide: effect of hydration. *J. Lipid Res.* 36: 1936–1944.

Thewalt, J. L., and M. Bloom. 1992. Phosphatidylcholine: cholesterol phase diagrams. *Biophys. J.* 63:1176–1181.

Veiga, M. P., M. J. R. Arrondo, F. M. Goni, and A. Alonso. 1999. Ceramides in phospholipid membranes: effects on bilayer stability and transition to nonlamellar phase. *Biophys. J.* 76:342–350.

Venkataraman, K., and A. H. Futerman. 2000. Ceramide as a second messenger: sticky solutions to sticky problems. *Trends Cell Biol.* 10: 408–412.

Vist, M., and J. H. Davis. 1990. Phase equilibria of cholesterol/dipalmitoylphosphatidylcholine mixtures: ^{2}H nuclear magnetic resonance and differential scanning calorimetry. *Biochemistry.* 29:451–464.

Wu, S. H., and H. M. McConnell. 1975. Phase separations in phospholipid membranes. *Biochemistry.* 14:847–854.

Xu, X., R. Bittman, G. Duportail, D. Heissler, C. Vilcheze, and E. London. 2001. Effect of the structure of natural sterols and sphingolipids on the formation of ordered sphingolipid/sterol domains (rafts): comparison of cholesterol to plant, fungal, and disease-associated sterols, and comparison of sphingomyelin, cerebrosides and ceramide. *J. Biol. Chem.* 276: 33540–33546.